Supporting Information

Sampah et al. 10.1073/pnas.1018360108

SI Methods

Generation of Drug-Resistant Mutants. A previously described HIV-1 NL4-3 proviral construct encoding GFP within a truncated *env* ORF (1) was a starting vector for the construction of mutant proviruses. In this construct, there is a KDEL sequence after the GFP coding sequence. This results in retention of GFP in the endoplasmic reticulum, giving high-level expression in infected cells. Fragments of this vector containing the relevant HIV-1 genes were cloned into pCR 4Blunt-TOPO vector. Site-directed mutagenesis was performed on the resulting vectors by PCR (QuikChange; Stratagene), according to the manufacturer's instructions, using primers coding for known single resistance mutations (2–4). The mutant fragment was then cloned into the complete NL4-3 vector to produce drug-resistant, GFP-tagged, envelope-defective HIV-1 vectors. The presence of the desired mutations in all recombinant HIV vectors was verified by DNA sequencing.

Clinical Isolates. Patient-derived *gag-pol* sequences were amplified by RT-PCR from plasma virus, as described previously (1), or by PCR from genomic DNA isolated from $CD4^+$ T cells that were infected with concentrated plasma from viremic patients. DNA sequencing confirmed that isolates only contained the M184V or K103N mutation. Recombinant HIV-1 vectors containing patient-derived *gag-pol* sequences were made by replacing a 1.5-kb *gag-pol* fragment of NL4-3 with corresponding patient-derived sequences.

Antiretroviral Drugs. We obtained RAL from Chemietek, EFV from Roche and elvitegravir from Gilead/Merck. All other anti–HIV-1 drugs were obtained through the AIDS Research and Reference Reagent Program, Division of AIDS, National Institute of Allergy and Infectious Diseases, US National Institutes of Health. All drugs were dissolved in DMSO at 60 mM, aliquoted, and stored at −20 °C, with the exception of tenofovir, TDF, emtricitabine, stavudine, EFV, and IDV, which were dissolved in double-distilled water. Drugs were serially diluted in their corresponding solvents to maintain the final solvent concentration in cell culture constant at 0.5% (vol/vol). Similar results were obtained for experiments using tenofovir and TDF.

Virus Production. HEK293T cells were cotransfected with the mutant NL4-3 vectors and an HIV-1 CXCR4 envelope expression vector using Lipofectamine 2000 (Invitrogen) according to the manufacturer's instructions. For experiments involving PIs, the medium was replaced with RPMI1640 (Invitrogen) supplemented with 50% (vol/vol) human serum (Gemini), 10% (vol/vol) FBS (Gemini), and serially diluted drugs 6–7 h after transfection. Virus-containing supernatants were collected after 48 h after transfection, spun at 335 × *g* for 10 min, and then filtered through a 0.22-mm membrane to remove cell debris. These virus preparations were then used for infection or stored at −80 °C. The amount of mutant virus used for each experiment was standardized relative to WT virus by measuring transfection efficiency of NL4-3 vector in the HEK293T cells using GFP expression as quantified by flow cytometry.

For all other drugs, transfected cells were cultured in RPMI1640 supplemented with 10% (vol/vol) FBS only. At 48 h after transfection, cell debris was cleared as described above and virus was harvested by ultracentrifugation at 100,000 × *g* at 4 °C for 2 h, aliquoted, and stored at −80 °C. The amount of mutant virus used for each experiment was standardized relative to WT virus by p24 concentration measured using an ELISA (Perkin–Elmer).

Single-Round Infectivity Assay. A single-round infectivity assay (1, 5, 6) was used to evaluate antiretroviral drug activity against drug-resistant variants. Peripheral blood mononuclear cells were obtained from healthy blood donors by Hypaque-Ficoll gradient centrifugation. All healthy blood donors gave their informed consent, and the Institutional Review Board of The Johns Hopkins University approved this study. The cells were activated with phytohemagglutinin (0.5 mg/mL) and IL-2 (100 U/mL) for 3 d. $CD4^+$ T lymphoblasts were selected using magnetic beads (Miltenyi) and seeded in a 96-well plate at 100,000 cells per well in RPMI1640 supplemented with 50% (vol/vol) human serum, 10% (vol/vol) FBS, IL-2 (100 U/mL), and cytokine-rich supernatant. Drugs other than PIs were added at this step and maintained throughout the culture. Standardized amounts of virus were added 16–18 h after the addition of drugs, and spinoculation was carried out at 1,200 × *g* at 30 °C for 2 h. After a 3-d incubation at 37 °C, cells were washed and fixed with 2% (vol/vol) formaldehyde. In all experiments, cells were considered positive if the level of green fluorescence was above the gate established with uninfected lymphoblasts from the same donor. Infectivity was quantified as the percentage of GFP^+ cells by FACS analysis (BD Bioscience).

Analysis of Dose–Response Curves. All data were obtained from at least three experiments with cells from different HIV-1–negative blood donors. IC_{50} and slope values were calculated as described by Shen et al. (5). Briefly, the fraction of infection events unaffected by the drug (f_u) was calculated as the percentage of GFP^+ cells in the presence of drug normalized by the percentage of GFP^+ cells without drug. IC_{50} and m values were calculated from each dose–response curve by fitting data to the median effect model (Eqs. **1** and **2**) through least-squares regression analysis. We calculated *IIP* with Eq. **3**. We corrected for nonlinear m and unintegrated virus at high concentrations of PIs and integrase inhibitors, respectively, as described by Shen et al. (5). Selective advantage was estimated by multiplying the ratio $f_{u(\text{mutant})}/f_{u(\text{WT})}$ at a given drug concentration by the replication capacity of mutant virus relative to WT in the absence of drug.

Statistical Analyses. Using Microsoft Office Excel 2007, we performed least-squares regression analysis and calculated mean values and SDs for IC_{50} and m and P values for changes in m and IC_{50}. Correlation coefficients for scatter plots relating fold change in IC_{50} to fractional change in *IIP* at C_{max} (Fig. 4) were also calculated using Microsoft Office Excel.

1. Zhang H, et al. (2004) Novel single-cell-level phenotypic assay for residual drug susceptibility and reduced replication capacity of drug-resistant human immunodeficiency virus type 1. *J Virol* 78:1718–1729.
2. Rhee SY, et al. (2003) Human immunodeficiency virus reverse transcriptase and protease sequence database. *Nucleic Acids Res* 31:298–303.
3. Shafer RW (2006) Rationale and uses of a public HIV drug-resistance database. *J Infect Dis* 194(Suppl 1):S51–S58.
4. Johnson VA, et al. (2009) Update of the drug resistance mutations in HIV-1: December 2009. *Top HIV Med* 17:138–145.
5. McMahon, MA et al. 2007. The HBV drug entecavir - effects on HIV-1 replication and resistance. *N Engl J Med* 356:2614–2621.
6. Shen L, et al. (2008) Dose-response curve slope sets class-specific limits on inhibitory potential of anti-HIV drugs. *Nat Med* 14:762–766.

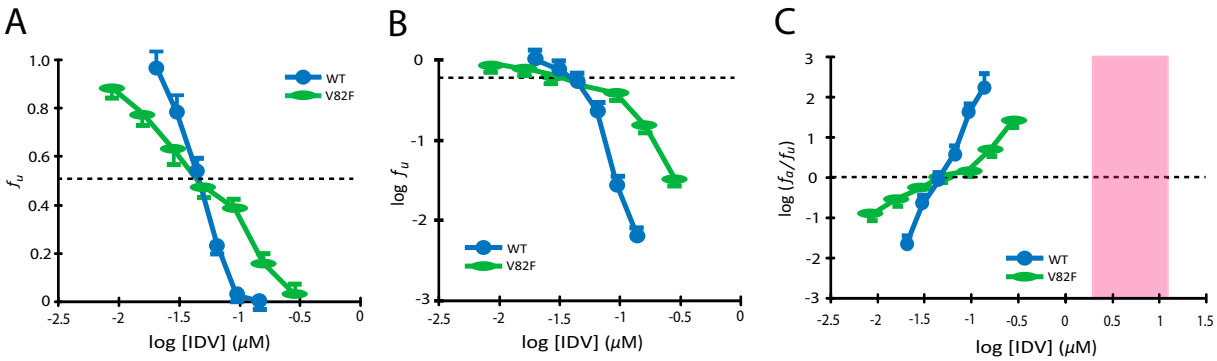

Fig. S1. V82F mutation in protease affects the slope but not the IC_{50} of the dose–response curve for IDV. (*A*) Standard semilog dose–response curve for WT virus and isogenic virus carrying the V82F mutation in protease. The dotted line represents 50% inhibition. (*B*) Log-log plot of the same dose–response data. The dotted line represents 50% inhibition. (*C*) Median effect plot of the same dose–response data. The dotted line represents 50% inhibition. The difference in the slopes is clearly evident. If the curves continue to diverge as the IDV concentration approaches the clinical concentration range (shaded area), the degree of inhibition of resistant virus may be as much as 5 log less than inhibition of WT virus.

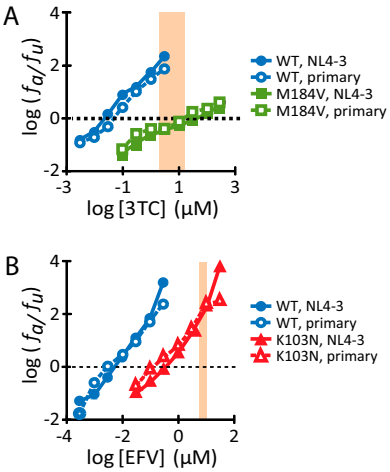

Fig. S2. Effect of resistance mutations on IC_{50} and *m* in primary isolates. (*A*) Effect of the M184V mutation on the response to 3TC. A primary isolate containing M184V as the only resistance mutation and an isogenic WT control generated by back-mutation of M184V were tested for susceptibility to 3TC. For purposes of comparison, median effect plots of dose–response curves for the WT (circles) and mutant (squares) forms of this primary isolate (open symbols, dotted lines) are overlaid on similar curves for the reference isolate NL4-3 (closed symbols, solid line) from Fig. 1*A*. (*B*) Effect of the K103N mutation on the response to EFV. A primary isolate containing K103N as the only resistance mutation and an isogenic WT control generated by back-mutation of K103N were tested for susceptibility to EFV. Results are plotted as described in *A*.

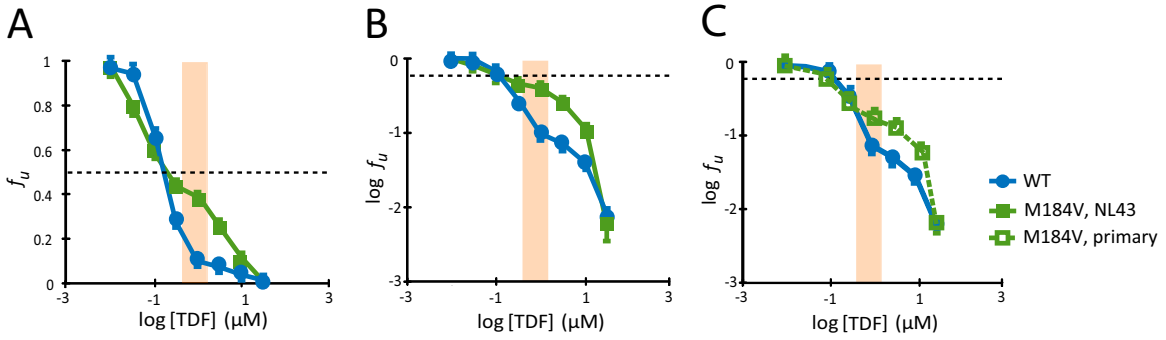

Fig. S3. Consideration of *m* reveals that the M184V mutation causes partial resistance to TDF. Semilog (*A*) and log-log (*B*) dose–response curves for the inhibition of infection by WT and M184V mutant NL43 viruses by increasing concentrations of TDF. Although the IC_{50} values for WT and mutant viruses are similar, the change in *m* makes the M184V virus resistant to TDF in the clinical concentration range (shaded area). (*C*) Log-log plot of the TDF dose–response curve against WT and M184V mutant virus preparations derived from a clinical isolate.

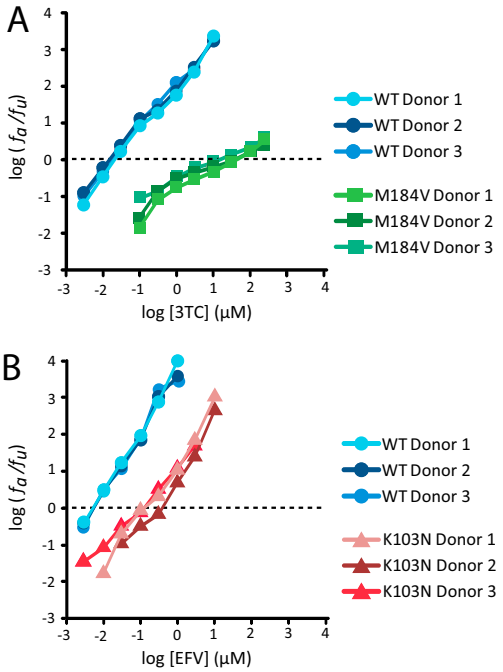

Fig. S4. Effect of donor-to-donor variability on the dose–response curve for 3TC and EFV against WT and resistant viruses. (*A*) Dose–response curves for 3TC against WT virus and virus carrying the M184V mutation. Primary CD4+ T lymphoblasts from three normal donors were infected with GFP-encoding HIV-1 pseudoviruses in the presence of increasing concentrations of 3TC, and infectivity was measured after 48 h by flow cytometry. Results are presented in the form of median effect plots to highlight the change in slope caused by the mutation. The dotted line represents 50% inhibition. The change in IC_{50} and slope caused by the M184V mutation was similar in all donors. (*B*) Dose–response curves for EFV against WT virus and virus carrying the K103N mutation obtained as described in *A*. The change in IC_{50} and slope caused by the K103N mutation was similar in all donors.

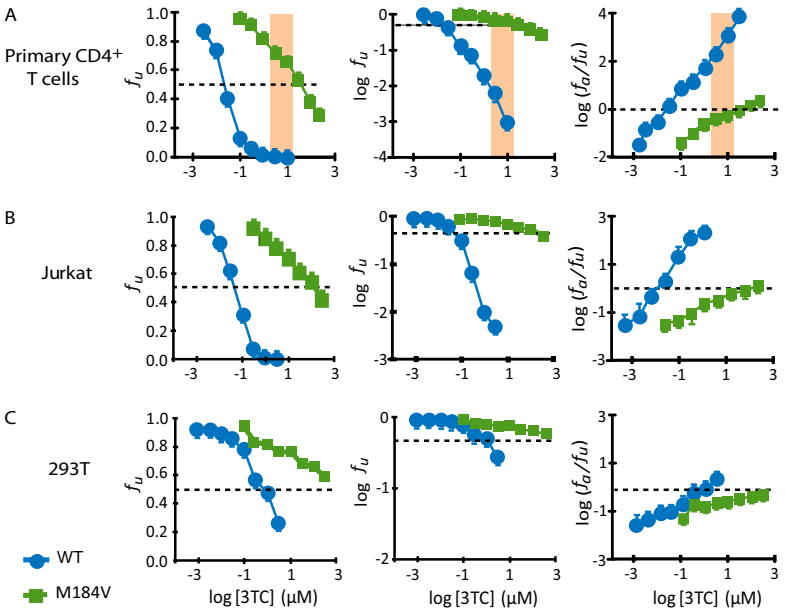

Fig. S5. Inhibition of WT and M184V mutant virus by 3TC in primary cells and cell lines. (*A*) Semilog (*Left*), log-log (*Center*), and median effect (*Right*) plots of the dose–response curve for 3TC against WT and M184V mutant virus in primary CD4+ T lymphoblasts. (*B*) Same plots of the dose–response curves for 3TC against WT and mutant virus in the Jurkat T-cell line. (*C*) Same plots of the dose–response curves for 3TC against WT and mutant virus in the human embryonic kidney cell line, 293T.

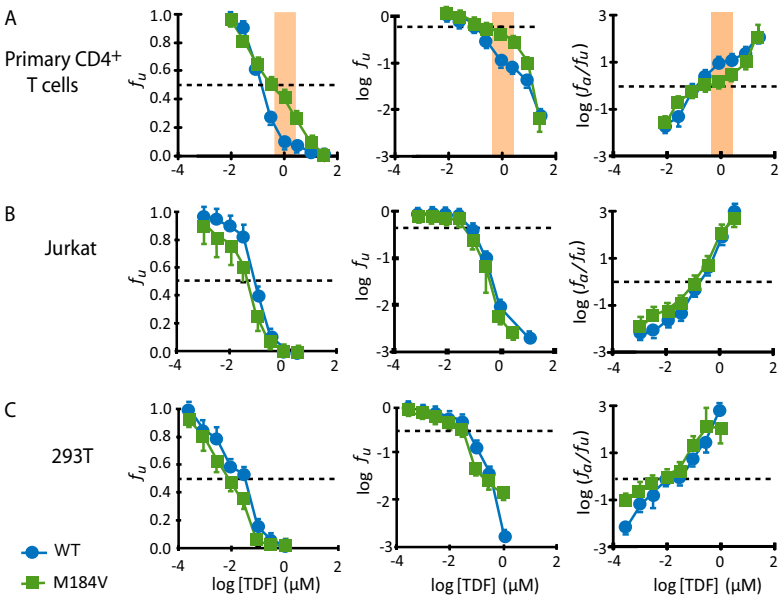

Fig. S6. Inhibition of WT and M184V mutant virus by TDF in primary cells and cell lines. (*A*) Semilog (*Left*), log-log (*Center*), and median effect (*Right*) plots of the dose–response curve for TDF against WT and M184V mutant virus in primary CD4$^+$ T lymphoblasts. (*B*) Same plots of the dose–response curves for TDF against WT and mutant virus in the Jurkat T-cell line. (*C*) Same plots of the dose–response curves for TDF against WT and mutant virus in the human embryonic kidney cell line, 293T.

Table S1. Glossary for abbreviations

f_a	Fraction of viruses or infection events affected by the drug
f_u	Fraction of viruses or infection events unaffected by the drug
D	Drug concentration
IC_{50}	Drug concentration that leads to 50% inhibition
m	Slope parameter or Hill coefficient
IIP	Instantaneous inhibitory potential, the log inhibition of single-round infectivity at clinical concentrations